Investigation of Heat Flow during MIG Welding of Stainless Steel 409M Plates and Prediction of Bead Parameters

Pradeep Khanna[1] and R. S. Parmar[2]

[1]Associate Professor, Department of Mechanical Engineering, NSUT, New Delhi, India.
[2]Former Professor, Department of Mechanical Engineering, IIT Delhi, India.
Email: pradeep.khanna@nsut.ac.in, 4.khanna@gmail.com

DOI : 10.22486/iwj.v53i4.203670

Dr. Pradeep Khanna : ORCID ID: https://orcid.org/0000-0002-1124-5981
Dr. R. S. Parmar : ORCID ID: https://orcid.org/0000-0003-3449-2560

Abstract

Nearly 90% of welding in the world is carried out by one or the other arc welding process, therefore it is imperative to discuss the aspect of heat flow and temperature distribution in arc welding.The knowledge of temperature distribution in plates during and after welding is necessary for predicting microstructure, calculating bead parameters, distortions and residual stresses. Thus, to achieve a weld of desired quality to perform in service satisfactorily, it is essential to know the temperature distribution during welding. In the present case, an arrangement of thermocouples was developed with microprocessor based electronic control which was successfully used to plot real time temperature graphs (thermal histories) during welding of plates at different input parameters. From these temperature plots, isotherms for different weldments were generated which were found helpful in determining the cooling rates. These weld isotherms were then used to estimate temperature at different points. These results were then compared with their estimated values calculated from empirical relations and were found to be in coherence with the experimental values within reasonable limits. The peak temperature values obtained from the thermal histories were used to approximately estimate the critical weld bead dimensions like penetration and weld width with the help of empirical relations and when compared with actual values, were found to be in good conformance.

Keywords: Arc welding; temperature distribution; thermocouples; temperature graphs; bead parameters.

1.0 Introduction

Analysis of thermal distribution during welding is of vital importance as it has a significant effect on microstructural changes, residual stresses, distortion and fatigue life of weld structure [1, 2]. During welding, the mode of heat flow from a limited zone of weld pool to the neighbouring solid metal is mainly the conduction [3]. The source of heat for the metal plates to be welded is heat from the arc and the heat from the molten metal droplets. Further, the heat received by the plates through molten droplets is decided by many factors like mode of metal transfer, size of droplets and finally the temperature of these droplets [4, 5].

A number of researchers have contributed in this field by investigating the thermal cycle produced during fusion welding and have further studied its effect on mechanical and metallurgical properties of the resulting welds. Rosenthal [6] claimed the credit of initiating a significant work by developing a powerful mathematical model to estimate the distribution of temperature during arc welding and investigating its effects on the thermophysical properties of the material. Goldak [7] contributed significantly through his investigation where the heat source was considered as Pseudo-Gaussian and the experimental results were used for the validation of the developed model. Gery et al. [8] carried out study to understand the effect of welding parameters like speed and heat input in combination with distribution of heat source on the variation of temperature. A proposal to consider heat source in a manner of Gaussian distribution from a moving point heat source was put forward by Pavelic [9]. Investigation

of the weld efficiency in relation with transient thermal properties was carried out by Little and Kamtekar [10]. Zhu and Chao [11] concluded that the transient temperature distribution fields are affected by the thermal properties of the material during welding. Dutta et al. [12] investigated the welded joints of high carbon steel for the effects of thermal parameters on the distribution of temperature during GTA process. Poorhaydari et al. [13] experimentally validated the empirical models for the determination of cooling rates and the maximum temperature attained in different thicknesses of steel plates. These studies have motivated the present work of undertaking the investigation of the heat flow during MIG welding and the prediction of bead geometry.

The kinetics of most welding processes is governed primarily by two factors- the heat generated by the electric arc and the heat dissipated by the metallic conduction [14]. The secondary heat dissipation by atmospheric convection and radiation may often be entirely neglected. Analytical methods have been in an attempt to find generalized solution to the problem and the results so obtained are sought to be checked for their accuracy by comparison with the experimental data. The temperature field in welding is assumed to be quasi–stationary which implies that the temperature over the plate remains same if the arc centre is considered as origin [15]. In simple words, under a condition of quasi – stationary state of heat flow, isotherms representing different temperatures remain at a fixed distance with respect to the heat source. Mathematically stated it means $\delta T/\delta t = 0$, where T is the temperature at any time and t is the time unit. Now, with any particular welding condition, the manner in which the temperature at a particular point in the weld pool varies with time will depend on the position of the point with respect to the source of heat, the welding arc [16]. The heat dissipation calculations may be used for predicting size of weld [14]. Rosenthal [17] proposed a formula to explain temperature field in a body subjected to an instant point heat source.

The present work is concerned with two-dimensional case identified with single weld run using bead on plate technique. In order to simplify the treatment, the assumption is made that the melting during welding is derived from the arc distributed uniformly through the thickness of the plate. An attempt has been made to draw the weld isotherms by recording the temperatures at different locations from the weld line with the help of thermocouples as shown in **Fig. 1**, where T_1, T_2, T_3, T_4 and T_5 represent the locations of thermocouples with respect to the weld centre line.

Temperatures at different randomly selected locations were then calculated through Rosenthal equation by using the data from the thermal histories plotted and compared with the experimentally obtained values. Also, important weld bead characteristics like weld penetration and weld width were calculated by using data from these thermal histories and were

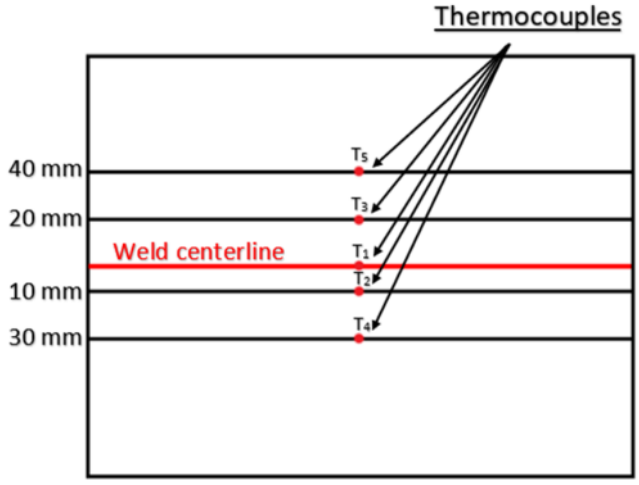

Fig. 1 : Location of the five thermocouples on the weld specimen

compared with actual values [18]. Good agreement was found between calculated and observed values.

2.0 Temperature distribution and weld bead estimation

The equation found suitable to calculate temperature at desired points on the surface of the weldment is given below [17],

$$T - T_0 = \frac{Q_P}{2\pi k} \cdot e^{-\lambda v x} \cdot \frac{e^{-\lambda v R}}{R} \qquad (1)$$

Where, T = temperature at the point of interest (°C)

T_0 = ambient temperature (°C)

Q_p = quantity of heat input (J/sec)

k = co efficient of thermal conductivity (J/m. sec. °C)

$\lambda = \frac{1}{2\alpha'}$ where α is thermal diffusivity (m^2/sec)

v = welding speed (m/sec)

$R = \sqrt{x^2 + y^2}$, where x and y are the coordinates of the point at which temperature is required to be determined with respect to the weld centre.

Using above equation, it is possible to determine temperature at any given point during quasi-stationary state of welding and from such a data it is possible to draw thermal histories for any point of interest. If sufficient number of such thermal histories is known for different points along a transverse section with respect to the weld centreline then such thermal histories can be used to draw isotherms for different temperatures keeping the weld pool periphery as the innermost isotherm representing the solidus temperature of the material being welded. From these isotherms, it is possible to determine the cooling rate in any direction. If such a cooling rate is

superimposed on the time-temperature-transformation curve of the material under consideration, then it becomes possible to predict the metallurgical transformations taking place in the heat affected zone along that direction; from which it may be possible to determine the mechanical strength of the weldment.

In the present case, a five-channel thermal sensing and recording unit has been developed in house as shown in **Fig. 2**, and was used to plot the real time thermal histories. The unit was calibrated by measuring the temperatures of known values like in this case three values were selected viz. temperature of melting ice, boiling water and molten sulphur at normal atmospheric conditions. The temperatures of these substances were measured a number of times by using the unit and compared with their known standard values i.e. 0°C, 100°C and 444°C respectively. It was found that the unit was giving satisfactory results with an average error of ±2.0%.

Based on Rosenthal's equation for heat flow, Christensen et. al [19]carried out experimental work which showed a good agreement between Rosenthal's point heat source-based solution and the actual weld bead geometry, under a wide range of welding conditions and material properties and have derived theoretical relationships between the weld dimensions and the welding conditions, using dimensionless parameters D and η which are related to each other as shown in **Fig. 3**, and can be expressed by the following relationships [4],

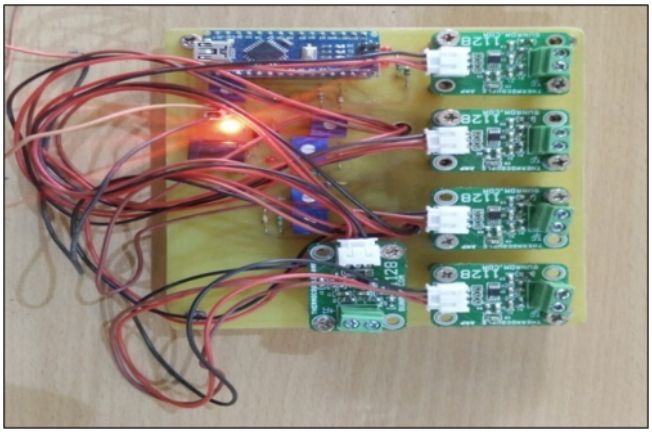

Fig. 2 : Five-channel thermal sensing and recording unit

$$\text{Dimensionless depth, } D = \frac{\rho . v}{2\alpha} \qquad (2)$$

and dimensionless operating parameter,

$$\eta = \frac{Q_p . V}{4\pi\alpha^2 \rho c (T_p - T_o)} \qquad (3)$$

Where,

p = weld penetration (mm)

T_p = peak temperature at given weld conditions, obtained from thermal history (°C)

ρ = density of the material being welded (kg/m^3)

c = specific heat (J/kg °C)

The linear energy is given by the following relation [4],

$$\text{Linear energy, } q_{lin} = \frac{q}{v} = \frac{0.241\ IV\eta}{v} \qquad (4)$$

Where,

q = heat input (cal/sec)

v = welding speed (cm/sec)

V = arc voltage (volts)

I = welding current (amps)

η = efficiency of heat transfer

and the weld width 'w' is given as [4],

$$w = \frac{0.484\ q_{lin}}{c\ \rho\ T\ \delta} \qquad (5)$$

Where,

T = peak temperature at given weld conditions, obtained from thermal history (°C)

Where,

T = peak temperature at given weld conditions, obtained from thermal history (°C)

δ = plate thickness (cm)

The values of different constants used in the above formulae are given below [20, 21],

T_0 = 20°C

ρ = 7700 kg/m^3

c = 459.8 J/kg °C

k = 25 J/m sec °C

α = 7 x 10^{-5} m^2/sec

η = 60%

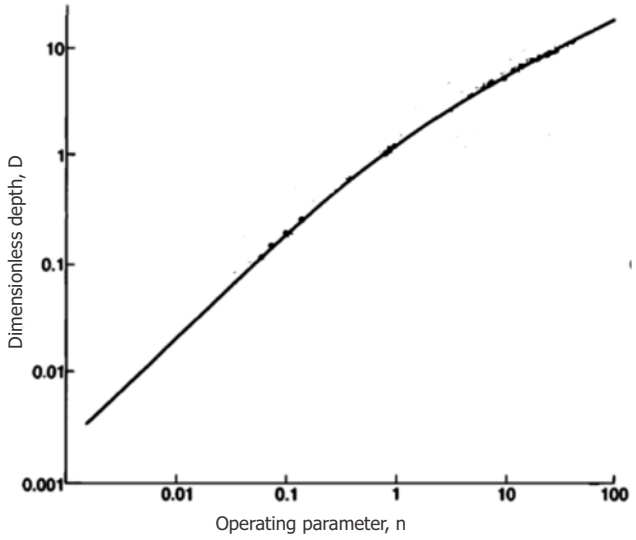

Fig. 3 : Relationship between dimensionless operating parameter n and the dimensionless weld depth, D [22]

From the aforementioned details, it is evident that the researchers in this field, aimed at using the well-known Rosenthal's equation of quasi-stationary state of heat flow during welding process. In spite of the claims made in their favour such mathematical models at their best appear to be nothing more than a tool for a rough estimation of the temperature field during welding process. Thus, if an accurate knowledge of the different aspects of the weld is to be gained, it is essential to carry out systematic experimental investigation to get a true picture of temperature histories so as to find a correlation between thermal, mechanical, metallurgical and physical effects (like bead shape, distortion). Hence it was decided to conduct a detailed experimental study to determine the trends in change of temperature during welding under different sets of parameters and to determine the effects of heat flow on bead shape by utilizing the data obtained from thermal histories and validate the same by comparing it with the observed values.

3.0 The experimental set up and procedure of experimentation

Having decided to follow the experimental technique, it was imperative to use proper welding system with requisite instrumentation to record or display the parameters of interest. The mechanized welding unit described earlier was utilized to achieve the desired welding speeds.

For welding, a constant voltage transformer cum rectifier with infinitely adjustable controls having an open circuit voltage of 18 to 60 volts was used. The maximum current capacity of the power source was 400 amps at 60% duty cycle. The wire feed unit coupled to the power source could provide wire feed rates in a range of 0 m/min to 22m/min through a step-less control.

Fig. 4 : The complete experimental set up

A built-in inductive reactance was available to control the amplitude of the welding current at the time of short circuit so as to control the extent of weld spatter. The welding torch was held in the torch holder of the welding unit. The open circuit voltage could be observed from the control panel of the power source. While the welding current and the arc voltage could be directly read-off from digital display of the welding machine panel. The complete set-up for carrying out the present study is shown in **Fig. 4**.

To record the thermal histories, it was decided to use five K-type thermocouples starting from weld centreline to either side at an incremental distance of 10 mm transverse to the weld centreline as shown in **Fig. 1**. K-type is the general-purpose thermocouples with a wide range of operating temperature, -260°C to 1260°C. They consist of chromel and alumel conductors [23]. Before connecting the hot junction of the thermocouples to the weld specimen; in order to ensure a good point contact, it was felt to fuse the two-thermocouple wire ends together. This was successfully done by melting and fusing the two wire ends in the form of a small nugget with the help of a soft carbon arc. Obviously, these thermocouples could be embedded into the test specimen from the backside only which was done by drilling 3mm diameter and 3mm deep holes at the preselected locations. These locations were then filled one after the other with silver brazing material and the fused hot junctions of the thermocouples were embedded in them as shown in **Fig. 5**.

Fig. 5 : Thermocouples brazed onto the weld specimen

The cold junctions were kept 1m away at ambient temperature to protect the recording zone against flying spatters. These five cold junction points of the thermocouples were connected to the in-house developed five channel thermal sensing and recording unit as shown in **Fig. 6** below.

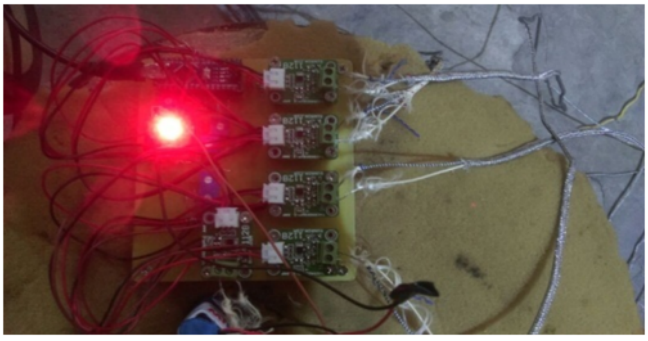

Fig. 6 : Five channel thermal sensing and recording unit with thermocouples connected

While welding the specimen with thermocouples attached at its back, it was imperative to keep them on some support. A stepped support was then developed to place the specimen on and which could give a clear gap of 100mm between the machine table and the backside of the specimen to accommodate the thermocouple wires. **Fig. 7** shows a close-up of one of the specimens supported on the stepped support, ready for welding.

Once the specimen was in position and the welding circuit completed, it remained to switch on the recording unit and to initiate the arc at the appropriate point. When the welding

Fig. 7 : The workpiece supported on stepped support

starts, thermocouples start sending output to the recording unit which consists of amplifiers, Wheatstone bridge and a microprocessor-based microcontroller, Arduino nano which performs the primary function of processing the data from the amplifier and transferring it to the computer. The program fed into the microprocessor then processes this input data and converts it to temperature values.

These data are then plotted as a function of time on the computer screen on real time basis. Recording was continued till the plate was sufficiently cooled down, thus, giving complete details of cooling profile for all the five points. The same procedure was repeated for all the specimens.

The welds were completed one after the other and all the five time-temperature graphs obtained simultaneously for each one of them were retained. The welding parameters used for these experiments are given in **Table 1**.

Table 1: Experimental values for different welding parameters

Specimen No. No.	WFR (m/min)	Welding speed (cm/min)	NPD (mm)	Voltage (V)	Torch Angle (degrees)
1	2.8	40	15	26	90
2	6.8	40	15	26	90
3	10.8	40	15	26	90
4	6.8	30	15	26	90
5	6.8	50	15	26	90
6	6.8	40	10	26	90
7	6.8	40	20	26	90
8	6.8	40	15	20	90
9	6.8	40	15	32	90
10	6.8	40	15	26	105
11	6.8	40	15	26	75

Industrially pure Argon gas was used for shielding and 1.2mm filler wire of stainless steel 308L was employed.

4.0 Results and Discussions

From the large number of time-temperature records, obtained for different welding parameters, eleven numbers of thermal histories were plotted. To keep the text within reasonable limits, only three are presented here (**figures 8-10**). From these thermal histories, peak temperatures were obtained which were utilized to calculate the important weld bead parameters like weld penetration and width by using equations (2-5). The results are given in **table-2**. It can be seen that the estimated and calculated values of penetrat ion and width are in good agreement within a reasonable limits of percentage errors.

Further, temperatures at randomly selected points A, B and C on the surface of the weldments were calculated by using equation (1). These results when compared with the actual values on the weld isotherm at the same points were found to be in good agreement, as shown in **table-3**. It can be seen that the estimated and calculated values of temperature are in good agreement within a reasonable limits of percentage errors.

Table 2 : Calculated and estimated weld bead parameters

Specimen No.	Peak Temp. (^{o}C)	Calculated penetration (mm)	Observed penetration (mm)	% error (mm)	Calculated width (mm)	Observed width (mm)	% error (mm)
1	975	1.74	1.7	-2.29	9.2	8.62	-6.3
2	1050	2.1	2.22	5.71	11.06	10.21	-7.68
3	1300	2.28	2.31	1.31	12.02	11.22	-6.65
4	1200	1.8	1.96	8.88	9.53	10.32	8.28
5	980	1.78	1.9	6.74	8.68	8.97	3.34
6	1200	1.8	1.96	8.88	9.53	10.32	8.28
7	950	2.03	1.9	-6.4	10.75	11.41	6.13
8	850	1.7	1.72	1.1	8.9	8.2	-7.86
9	1200	2.37	2.23	-5.9	12.45	12.43	-0.16
10	900	1.72	1.84	6.97	10.63	10.72	0.84
11	1050	2.03	1.95	-3.94	9.11	9.58	5.15

Table 3 : Calculated and estimated values of temperature

POINT A			POINT B			POINT C		
Calculated Temperature (^{o}C)	Observed Temperature (^{o}C)	% Error	Calculated Temperature (^{o}C)	Observed Temperature (^{o}C)	% Error	Calculated Temperature (^{o}C)	Observed Temperature (^{o}C)	% Error
625.4	600	-4.06	385.5	400	3.76	276.5	300	8.4
508.7	500	-1.71	488.3	500	2.39	288.6	300	3.95
626	600	-4.15	332	300	-9.63	576.2	600	4.13
585	600	2.56	458	500	9.17	247.6	250	0.96
660.3	600	-9.13	465.4	500	7.43	263.2	250	-5.01
868	800	-7.83	559.3	600	7.27	363.7	400	9.98
841.6	900	6.93	547.5	600	9.58	466.8	450	-3.59
480	500	4.16	318.6	300	-5.83	268.6	250	-6.92
947.6	900	-5.02	616.7	600	-2.7	322.1	300	-6.86
554.6	600	8.18	532.2	500	6.05	279.3	300	7.41
566.4	600	5.93	424.5	400	-5.77	331.8	300	-9.5

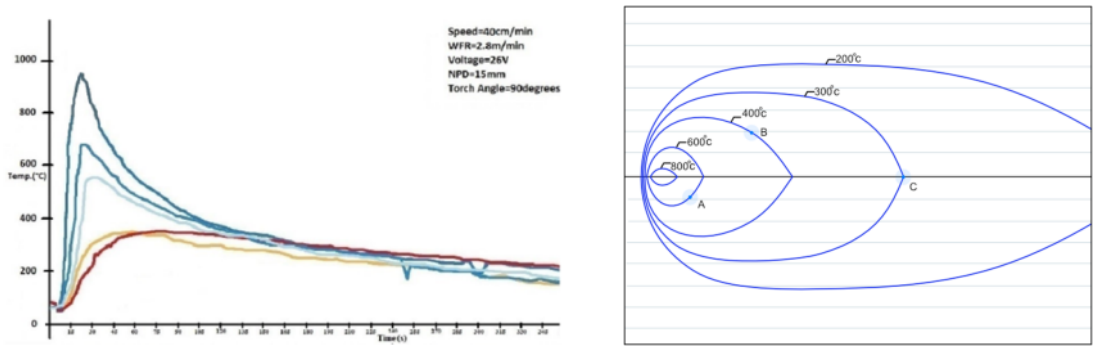

Fig. 8 : Thermal histories and weld isotherm diagrams for specimen # 1

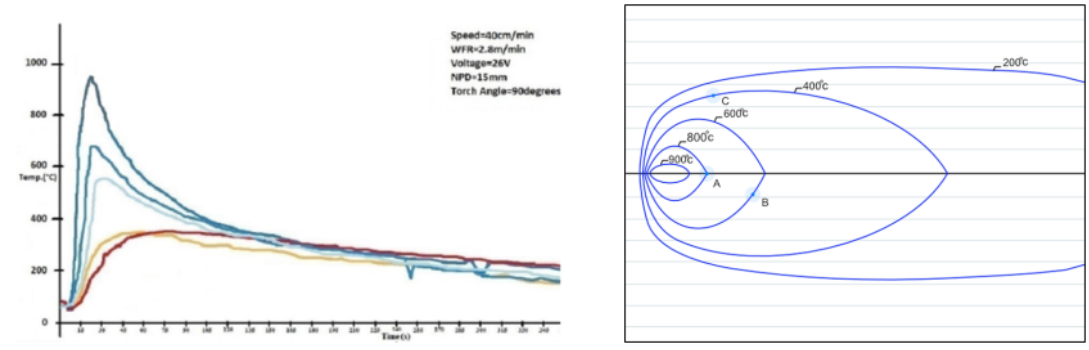

Fig. 9 : Thermal histories and weld isotherm diagrams for specimen # 6

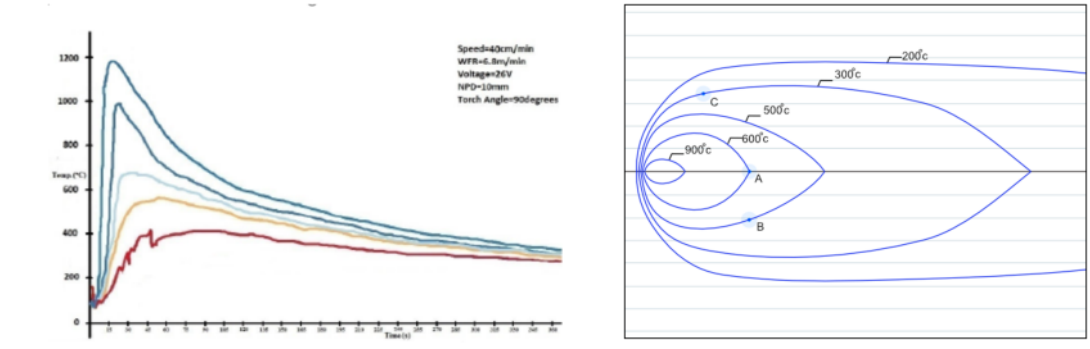

Fig. 10 Thermal histories and weld isotherm diagrams for specimen # 10

Figures 11, 12 and **13** are the scatter diagrams plotted to show the deviations between calculated and actual values of penetration, weld width and surface temperatures respectively. It is evident from these figures that there is good amount of agreement between the calculated and the actual values. These diagrams further prove the validity of mathematical equations utilized to calculate the values of penetration, weld width and surface temperatures for welds made under different sets of parameters.

Study of heat flow in welding thus provides an alternate and reliable method to calculate important weld bead dimensions without actually measuring them, thereby saving considerably the effort and time going into specimen preparation and measurement. The weld isotherms plotted on the basis of thermal histories also have been found to be fairly accurate to know the temperature at any desired location on the weldment without actually calculating it, thereby saving considerable calculation time and effort.

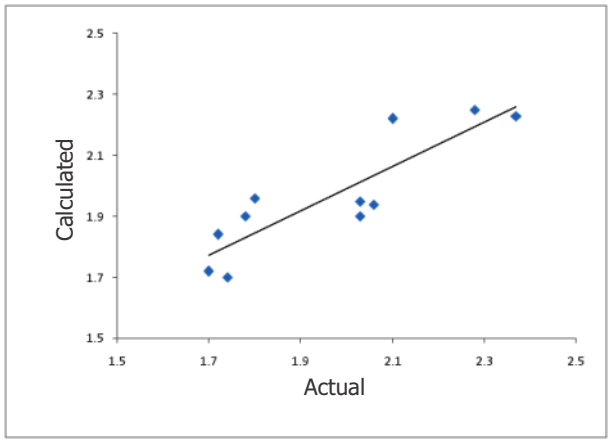

Fig. 11 : Scatter diagram for actual Vs calculated values of penetration

These weld isotherms can therefore be used directly to know the temperature and cooling rates at the point and in the direction of interest. The cooling rates obtained from the weld isotherms when superimposed on the time-temperature-transformation curve of the material under consideration, can help predicting the microstructure formed under different cooling rates. The information so obtained can be used to estimate the mechanical strength of the weldment and consequently the service behaviour of the welded structure.

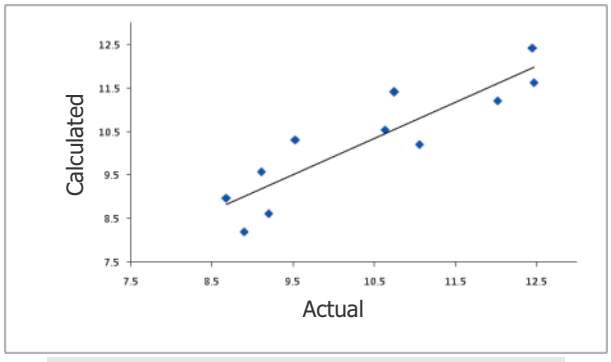

Fig. 12 : Scatter diagram for actual Vs calculated values of width

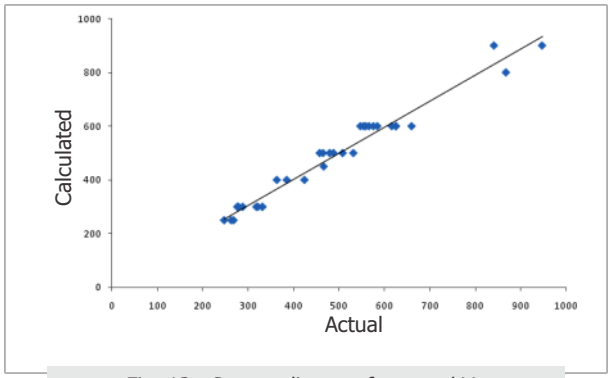

Fig. 13 : Scatter diagram for actual Vs calculated values of temperature

5.0 Conclusions

Study of heat flow provided a fairly reliable alternative to determine important weld bead dimensions when compared to actual measurements. It also helped to plot thermal histories of welds made at different conditions, which were found useful in understanding the temperature distribution, determining the cooling rates and calculating the temperature at any point on the isotherm curves. It was found that the calculated and observed value of temperature, depth of penetration and weld width were in good agreement with the actual measured values thereby proving the worth and usefulness of the work carried out.

References

[1] Negi V, Chattopadhyaya S (2013); Critical assessment of temperature distribution in submerged arc welding process, Advances in Materials Science and Engineering, pp. 1-9.

[2] Arora H, Singh R, Brar GS (2019); Thermal and structural modelling of arc welding processes: a literature review, Journal of Measurement and Control, 52(7-8), pp. 955-969.

[3] Boob AN, Gattani GK (2013); Study on effect of manual metal arc welding process parameters on width of heat affected zone (HAZ) for sae 1005 steel, International Journal of Modern Engineering Research, 3(3), pp. 1493-1500.

[4] Parmar RS (2010); Welding Engineering and Technology, 2nd edition, Khanna Publishers, Delhi.

[5] Das R, Bhattacharjee K S and Rao S (2012); Welding heat transfer analysis using element free Galerkin method, Advanced Materials Research, 410, pp. 298-301.

[6] Rosenthal D (1946); The theory of moving heat sources and its applications in metal treatments, Transactions of the ASME, 68, pp. 849-865.

[7] Goldak JA (1997); Thermal stress analysis in solids near the liquid region in the welds: mathematical modelling of the weld phenomena, The Institute of Materials, pp. 543-570.

[8] Gery D, Long H, Maropoulos PG (2015); Effect of welding speed, energy input and heat source distribution on temperature variations in butt joint welding, Journal of Materials Processing Technology, 167, pp. 393-401.

[9] Pavelic V (1969); Experimental and computed temperature histories in gas tungsten arc welding of thin plates, Welding Journal, Research Supplement, 48, pp. 295s-305s.

[10] Little GH, Kamtekar A G (1998); The effect of thermal

properties and weld efficiency on transient temperatures in welding, Computers and Structures, 68, pp. 157-165.

[11] Zhu XK, Chao YJ (2012); Effects of temperature dependent material properties on welding simulation, Computers and Structures, 80 pp. 967-976.

[12] Dutta J, Narendranath S (2014); Experimental and analytical investigation of thermal parameters developed in high carbon steel joints formed by GTA welding, Journal of Mechanical Engineering, 44 (2), pp. 88-86.

[13] Poorhaydari K, Patchett BM, Ivey DG (2016); Estimation of cooling rates in the welding of plates with intermediate thickness, Welding Journal, Research Supplement, pp. 148s-155s.

[14] Wells A (1952); Heat flow in welding, Welding Journal, Research Supplement, 31(5), pp. 263s -267s.

[15] Gupta BD, Gupta OP (1978); Temperature distribution in fillet welds, J of the Institution of Engineers (India), 59(2), pp. 87-92.

[16] Sterenbogen AY (1964); Weld pool solidification, E. O. Paton Welding Institute, Avt. Svarka, Ukraine, 10, pp. 20-25.

[17] Rosenthal D (1941); Mathematical theory of heat distribution during welding and cutting, Welding Journal, Research Supplement, pp. 220s-234s.

[18] Ismail MIS, Afieq W M (2016); Thermal analysis on a weld joint of aluminium alloy in gas metal arc welding, Advances in Production Engineering and Management, 11(1), pp. 29-37.

[19] Christensen N, Davies V, Gjermundsen K (1965); Distribution of temperature in arc welding, British Welding Journal, 12(2), pp. 54-75.

[20] Jindal Stainless Products data-sheets for different grades, 2016.

[21] Salem Stainless, User's Guide, 2012.

[22] Lancaster JF (1980); Metallurgy of Welding, 3rd edition, George Allen and Unwin, London.

[23] www.tempsens.com accessed on 26.08.2020.